Chemical Engineering & Processing: Process Intensification 183 (2023) 109214

Contents lists available at ScienceDirect

Chemical Engineering and Processing - Process Intensification

journal homepage: www.elsevier.com/locate/cep

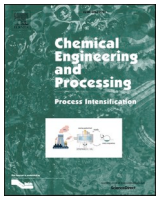

Multi-walled carbon nanotubes as a platform for Immunoglobulin G attachment

Mafalda R. Almeida [a], Rita A.M. Barros [b,c], Matheus M. Pereira [a], Daniel Castro [a], Joaquim L. Faria [b,c], Mara G. Freire [a], Cláudia G. Silva [b,c,*], Ana P.M. Tavares [a,*]

[a] CICECO - Aveiro Institute of Materials, Department of Chemistry, University of Aveiro, Aveiro, Portugal
[b] LSRE-LCM - Laboratory of Separation and Reaction Engineering - Laboratory of Catalysis and Materials, Faculty of Engineering, University of Porto, Rua Dr. Roberto Frias, 4200-465, Porto, Portugal
[c] ALiCE - Associate Laboratory in Chemical Engineering, Faculty of Engineering, University of Porto, Rua Dr. Roberto Frias, 4200-465, Porto, Portugal

ARTICLE INFO

Keywords:
Antibodies
Immunoglobulin G
Attachment
Computational analysis
Multiwalled carbon nanotubes

ABSTRACT

Nanomaterials have been extensively used in different applications due to their peculiar characteristics and nanoscale dimensions. Among nanoparticles, carbon-based nanomaterials are becoming highly attractive for biomedical applications such as diagnosis, tissue engineering, drug delivery, and biosensing. The conjugation of carbon-based nanomaterials with antibodies combines the properties of these materials with the specific and selective recognition ability of the antibodies to antigens. The present work proposes a process intensification approach for immunoglobulin G (IgG present in rabbit serum) attachment on multi-walled carbon nanotubes (MWCNTs) in a single step. The effect of several parameters, namely MWCNTs external diameter, rabbit serum concentration, MWCNTs functionalization and pH value, on the IgG attachment yield was evaluated. The dilution of rabbit serum decreased other protein attachment, namely rabbit serum albumin (RSA), while increasing the IgG yield to 100%. The interaction mechanisms between IgG and MWCNTs were evaluated at pH 5.0 to 8.0. The protonation of IgG amino acids indicates that N-term are the most reactive amino acids in the antibody structure. The identification of the N-term reactivity at pH 8.0 allows to indicate a possible orientation of the antibody over the MWCNTs surface, described as "end-on". Since the amount of RSA attached to MWNT decreased with the increase in serum dilution, the IgG orientation and amine activity was not affected. This orientation demonstrates that the IgG attachment over the surface of the MWCNTs could be an effective strategy to maintain the antigen recognition by the antibody, and to be used for biomedical applications.

1. Introduction

Carbon nanotubes (CNTs) consist entirely of carbon atoms connected through sp^2 bonds structured in several condensed benzene rings rolled up into a cylinder form, presenting lengths in the order of μm and diameters up to 100 nm [1]. Depending on the process for CNTs fabrication and the number of graphitic layers, CNTs are classified into single-walled carbon nanotubes (SWCNTs) or multiwalled carbon nanotubes (MWCNTs). SWCNTs own the simplest morphology, consisting of a single layer of graphene with diameters between 0.4 and 2 nm, generally existing as hexagonal close-packed bundles, while MWCNTs comprise two or more concentric cylinders, each made of a single graphene sheet surrounding a hollow core with inner diameters between 1 and 3 nm [2]. CNTs have specific structural properties [3], strong loading capacity [4], biocompatibility [5], high surface area, high strength, and enhanced chemical and thermal stability [6], and therefore have been highly applied in the biomedical, biosensing and biotechnological fields [7–9]. The conjugation of different biomolecules to the CNTs widens their application fields and provides them with new or enhanced properties [10]. A range of biomolecules have been conjugated with CNTs, including peptides [11,12], proteins [13,14], antibodies [15,16], enzymes [17,18] and DNA [19]. Most of these biomolecules have shown several advantages when linked to the nanomaterial, such as the ability of crossing biological membranes [10].

The conjugation of CNTs with antibodies combines the properties of the carbon-based nanomaterials themselves with the specific and selective recognition ability of the antibodies to antigens, and so have been applied in two biomedical fields: therapy and diagnosis. In therapy, in

* Corresponding authors.
E-mail addresses: cgsilva@fe.up.pt (C.G. Silva), aptavares@ua.pt (A.P.M. Tavares).

https://doi.org/10.1016/j.cep.2022.109214
Received 28 February 2022; Received in revised form 14 November 2022; Accepted 17 November 2022
Available online 20 November 2022

the development of targeted drug delivery and tissue repairing; and in diagnosis, as contrast agents for magnetic resonance imaging (MRI), sensing, cell sorting, bioseparation, enzyme immobilization, immunoassays, transfection (gene delivery), and purification [10]. To conjugate the antibodies to CNTs, two different strategies have been described, namely covalent bonding [20,21] and noncovalent interaction [22]. However, a noncovalent interaction between the antibody and the CNTs may lead to conjugates with lower stability and selectivity. On the other hand, a covalent bond does not present this limitation and it offers, in addition, good stability and better binding selectivity due to its ability to directly control the location of the antibody.

Different authors reported several studies on the conjugation of antibodies with CNTs using various types of CNTs, antibodies, conjugation strategies and distinct applications. Venturelli et al. [23] reported the covalent conjugation of anti-MUC1 antibody on two different types of CNTs, namely MWCNTs and double-walled carbon nanotubes (DWCNTs). The authors coupled the antibody at the tops and at defect sites of the CNT backbone via direct amidation between the antibody and oxidized-CNTs, or onto their sidewalls via 1,3-dipolar cycloaddition, exploiting a selective chemical bonding based on the addition of thiolated antibody to maleimide-functionalized CNTs. Among all the bioconjugates prepared and analyzed, the MWCNT-based ones displayed the highest degree of aqueous dispersibility, and formed stable homogeneous dispersions under physiological conditions that render them useful for biomedical investigations. Li et al. [20] also described the use of an antibody covalently linked to CNTs. However, in this case, a P-gp antibody (anti-P-gp) was covalently bonded onto the oxidized single-walled carbon nanotubes (o-SWNTs) via a diimide-activated amidation reaction, with the goal of challenging the multidrug resistance of human leukemia K562R cells by recognizing the membrane P-gp of those cells. Additionally, Huang et al. [16] immobilized anti--*Salmonella* and anti-*Staphylococcus aureus* rabbit antibodies on hydrophobic and hydrophilic nanodiamond and CNTs coated silicon substrates. The results demonstrated a distinct antibody immobilization on the surface of hydrophobic and hydrophilic CNTs, with the air plasma treated nanodiamond having a higher efficacy for the antibody immobilization [16].

In the present work, pristine MWCNTs and MWCNTs functionalized through a simple hydrothermal oxidation procedure were used for the attachment of immunoglobulin G (IgG, polyclonal antibody) from commercial rabbit serum (containing IgG and other proteins naturally present, namely rabbit serum albumin (RSA)). This complex matrix was selected as the antibody source to prove the efficiency of MWCNTs in the adsorption of IgG [24]). The effect of several parameters, namely MWCNTs external diameter, rabbit serum concentration, MWCNTs functionalization and pH of serum, on the IgG attachment yield was evaluated. In addition, to confirm the strong interaction between IgG and the MWCNTs, and the potential of the bioconjugate for biomedical applications, different desorption strategies were applied, and the non-desorption of IgG verified. Moreover, to identify the interaction mechanisms between IgG and MWCNTs a computational analysis including a protonation analysis was performed. This work contributes to process intensification since it reports novel experimental data on the conjugation of multiwalled carbon nanotubes for the strong attachment of IgG in a single and simple step.

2. Materials and methods

2.1. Reagents and compounds

Rabbit serum (USDA approved) was purchased from Sigma-Aldrich.

Citrate/phosphate buffers were prepared using citric acid (99.5% of purity) and sodium phosphate dibasic heptahydrate (98.0-102.0% of purity) supplied by Panreac and Sigma-Aldrich, respectively. Phosphate buffers were prepared using sodium phosphate dibasic heptahydrate (98.0-102.0% of purity) and sodium phosphate monobasic (99-100.5% of purity) from Sigma-Aldrich and Panreac, respectively. Carbonate buffer was prepared with sodium hydrogencarbonate (≥99.7% of purity) and sodium carbonate anhydrous (99.9% of purity) from Merck and Prolabo.

Sodium chloride (99.5% of purity), hydrochloric acid (37% of purity) and phosphate-buffered saline (PBS) pH 7.4, were used in the back-extraction assays and supplied by Panreac, Fisher Scientific and Sigma-Aldrich, respectively.

For the size exclusion high-performance liquid chromatography (SE-HPLC), sodium phosphate dibasic heptahydrate (98.0-102.0% of purity), sodium dihydrogenphosphate (99% of purity) acquired from Sigma-Aldrich, and sodium chloride (99.5% of purity) from supplied by Panreac were used.

2.2. MWCNTs preparation

MWCNTs with different external diameter ranges (<10, 10-20, 20-40 or 60-100 nm), synthesized by chemical vapor deposition, were purchased from Shenzhen Nanotechnolo-gies Co. Ltd. (≥95% of purity, length= 5-15mm, ash content ≤0.2 wt%, amorphous carbon <3%). According to Silva et al. [18], MWCNTs with a diameter range of 10-20 nm were functionalized by heating them at reflux with HNO_3 (7M) at 130 °C (MWCNTox) to introduce oxygen functionalities. Then, the MWCNTox material was treated under an inert atmosphere (N_2) at 400 °C (MWCNTox 400) and at 900 °C (MWCNTox 900), to selectively remove surface groups. The surface area of the MWCNTs with different external diameter ranges were previously determined [18] and are presented in the Supporting Information, Table S1.

2.3. Optimization of the attachment of immunoglobulin G from rabbit serum on MWCNTs

The attachment of IgG present in rabbit serum over MWCNTs was carried out by direct physical adsorption in a batch system. The influence of several parameters, namely MWCNTs external diameter, rabbit serum dilution, MWCNTs functionalization and pH, was evaluated, and reported in terms of IgG attachment yield.

The effect of different MWCNTs external diameter ranges, namely <10, 10-20, 20-40 or 60-100 nm, on IgG attachment was firstly evaluated. For this, 100 μL of 0.15 M citrate/phosphate buffer pH 5.0 and 100 μL of diluted rabbit serum (1:30) were added to 2 mg of MWCNTs. The mixtures were stirred for 60 min in an orbital shaker, and then centrifuged for 10 min at 12000 rpm to separate the supernatant from the bioconjugate (IgG@MWCNT). A control was prepared with 0.15 M citrate/phosphate buffer pH 5.0 and 100 μL of diluted rabbit serum (1:30).

The influence of rabbit serum's dilution on IgG attachment was also investigated. For this, 100 μL of 0.15 M citrate/phosphate buffer pH 5.0 and 100 μL of diluted rabbit serum (1:5, 1:15, 1:20, 1:30 and 1:50) were added to 2 mg of MWCNTs 10-20 nm. As previously described, the mixtures were stirred for 60 min in an orbital shaker, and then centrifuged for 10 min at 12000 rpm to separate the supernatant from the bioconjugate (IgG@MWCNT). A control was prepared by adding 100 μL of 0.15 M citrate/phosphate buffer and 100 μL of diluted rabbit serum (1:5, 1:15, 1:20, 1:30 and 1:50).

Then, the MWCNT functionalization on IgG immobilization was studied. Therefore, 100 μL of 0.15 M citrate/phosphate buffer pH 5.0 and 100 μL of diluted rabbit serum (1:20) were added to 2 mg of different MWCNTs (MWCNT, MWCNTox, MWCNTox 400 and MWCNTox 900). The mixtures were stirred for 60 min in an orbital shaker, and then centrifuged for 10 min at 12000 rpm to separate the supernatant from the bioconjugate (IgG@MWCNT). A control sample was prepared with 100 μL of 0.15 M citrate/phosphate buffer and 100 uL of diluted rabbit serum (1:20).

Finally, the pH effect on IgG immobilization was evaluated. 100 μL of 0.15 M citrate/phosphate buffer pH 5.0 or 0.2 M phosphate buffer at pH values of 6.0, 7.0 and 8.0; and 100 μL of diluted rabbit serum (1:20),

were added to 2 mg of MWCNTox. The mixtures were stirred for 60 min in an orbital shaker, and then centrifuged for 10 min at 12000 rpm to separate the supernatant from the bioconjugate (IgG@MWCNT). A control sample was prepared with 100 μL of 0.15 M citrate/phosphate buffer or 0.2 M phosphate buffer at pH values of 6.0, 7.0 and 8.0, and 100 μL of diluted rabbit serum (1:20).

Size exclusion-high performance liquid chromatography (SE-HPLC) was used for the quantification of IgG and other proteins (RSA) present in the rabbit serum and in supernatants after IgG attachment. A calibration curve was determined for this purpose using commercial IgG from rabbit. A 50 mM phosphate buffer containing NaCl (0.3 M) was used as mobile phase. Each sample was diluted 1:9 (v:v) in the phosphate buffer and then injected on a Chromaster HPLC system (VWR Hitachi). The SE-HPLC run was performed on an analytical column Shodex Protein KW802.5 (8 mm × 300 mm). The mobile phase run isocratically with a flow rate of 0.5 mL/min with an injection volume of 25 μL. The column oven and autosampler temperatures were kept at 40°C and 10°C, respectively. The wavelength was set at 280 nm using a DAD detector. The obtained chromatograms were analyzed using the PeakFit version 4 software.

The IgG attachment yield was calculated according to Eq. (1):

$$IgG\ attachment\ yield\ (\%) = 100 - \left(\frac{IgG\ peak\ supernatant\ area}{IgG\ peak\ rabbit\ serum\ area} \times\ 100\right) \quad (1)$$

where "*IgG peak supernatant area*" corresponds to the peak area of IgG in the supernatant after the IgG attachment and the separation of the bioconjugate by centrifugation, and "*IgG peak area*" is the peak area of IgG in the initial rabbit serum diluted according to the dilution in each assay.

The RSA attachment yield was calculated according to Eq. (2):

$$RSA\ attachment\ yield\ (\%) = 100 - \left(\frac{RSA\ peak\ supernatant\ area}{RSA\ peak\ rabbit\ serum\ area} \times\ 100\right) \quad (2)$$

where "*RSA peak supernatant area*" corresponds to the peak area of RSA in the supernatant after the RSA attachment, and "*RSA peak area*" is the peak area of RSA in the initial rabbit serum diluted according to the dilution in each assay.

2.4. Evaluation of the desorption of Immunoglobulin G from MWCNTs

To prove the strong interaction between the IgG and the MWCNTs, and the potential of this bioconjugate for biomedical applications, some assays were performed in an attempt to verify if IgG is easily desorbed or not from the MWCNTs. For these studies, 100 μL of 0.2 M phosphate buffer at pH 8.0 and 100 μL of diluted rabbit serum (1:20) was added to 2 mg of MWCNTox (best attachment conditions). After 60 min in an orbital shaker, the mixtures were centrifuged for 10 min at 12000 rpm and the supernatant was separated from the bioconjugate (IgG@MWCNTox). Different solutions (200 μL) at different pH values were added to the IgG@MWCNTox bioconjugates: 0.15 M citrate/phosphate buffer at pH 4.0, 5.0 and 6.0; 0.2 M phosphate buffer at pH 7.0 and 8.0; 0.5 M carbonate buffer at pH 9.0 and 11.0; PBS pH 7.4; sodium chloride aqueous solution (1.0 M, 1.5 M, 2.0 M, 2.5 M); 0.15 M citrate/phosphate at pH 2.8 with sodium chloride (0.5 M); and water with HCl at pH 2.8. The mixtures were stirred for 120 min in an orbital shaker and then centrifuged for 10 min at 12000 rpm to separate the supernatant from the bioconjugate. All the supernatants were analyzed by SE-HPLC as previously described.

2.5. Computational analysis

IgG protonation states of titratable residues were calculated using ProteinPrepare (PlayMolecule web server - playmolecule.org) [25]. IgG PDB file (PDB: 1hzh) was download from Protein Data bank and uploaded in ProteinPrepare application. The pK_a calculation was performed at pHs 5.0 to 8.0, without water molecules and ligands from input PDB file. After the calculation was performed, the protonated PDB files and protonation tables were downloaded and analyzed. IgG electrostatic surface were calculated using automatically-configured sequential focusing multigrid calculation on Adaptive Poisson-Boltzmann Solver (APBS). After refinement of pK_a values calculated, the reactivity of amino acids residues was identified using Ligand Interacting Groups Reactivity (*LIGRe*) [26]. *LIGRe* was calculated using Eq. (3):

$$LIGRe = 10^{(pH-pKa)} \quad (3)$$

where "*pH*" is the pH experimentally studied and "*pKa*" represents the acidic constant of the analyzed amino acid residue from IgG.

2.6. Transmission electron microscopy

Scanning transmission electron microscopy (TEM) was carried out using a HITACHI SU-70 high-resolution scanning electron microscope, equipped with a Bruker EDS detector. High-resolution transmission electron microscopy (HRTEM) was performed in a JEOL 2200FS transmission electron microscope, equipped with Oxford EDS detector and in-column omega filter.

3. Results and discussion

3.1. Attachment of Immunoglobulin G present in rabbit serum on MWCNTs

The capacity of MWCNTs to adsorb IgG (IgG@MWCNT) from rabbit serum was ascertained, and several parameters, namely MWCNTs external diameter, rabbit serum dilution, MWCNTs functionalization and pH value, were optimized in order to improve the IgG attachment yield. Considering that 1 mL of rabbit serum has approximately 7.66 mg mL^{-1} of IgG [27], it was possible to estimate the number of IgG molecules present in the initial samples of all rabbit serum dilutions used in this work (100 μL). Moreover, the theoretical maximum number of IgG able to be adsorbed on MWCNTs was estimated based on the surface area of the MWCNTs and the surface area covered by a single IgG in the different possible orientations [28]. Results are shown in Tables S2 and S3 (Supporting Information).

Fig. 1 shows the influence of the external diameter of MWCNTs on the IgG attachment yield from rabbit serum after the adsorption process. Regarding the results, the MWCNT with an external diameter range between 60-100 nm showed the poorest results with an IgG attachment yield of 45.9 %, which corresponds to a number of IgG molecules adsorbed of 2.82 × 10^{13}. This lower value is probably due to the large

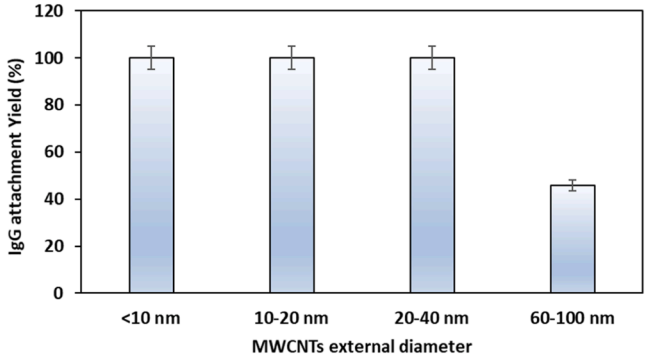

Fig. 1. Effect of MWCNTs external diameter in the attachment of IgG present in rabbit serum (1:50 diluted with 0.15 M citrate/phosphate buffer pH 5.0) on 2 mg of MWCNTs during 60 min of contact time.

diameter of the nanomaterial, which reduces the external surface area of the nanotubes (Table S1) and decrease the antibody adsorption [18]. On the other hand, the MWCNTs with lower external diameters range (<10, 10-20 and 20-40 nm) were more effective, presenting a complete IgG adsorption (IgG attachment yield of 100%), corresponding to 6.14×10^{13} IgG molecules. It has been reported that a bigger CNT curvature may help to reduce denaturing interactions between the protein and the CNTs [29] through the suppression of lateral interactions between adjacent adsorbed proteins. This can explain the higher activity of IgG attached on the MWCNTs with the smallest diameter range even in the presence of other proteins, naturally present in rabbit's serum. Besides, as shown in previous studies [18], the high surface area shown by the MWCNTs with the lowest diameter can also be a crucial parameter contributing to the antibody adsorption capacity increase and, hence, the efficient loading of IgG along the MWCNTs surface. Considering these results, MWCNTs with an external diameter of 10-20 nm were selected for the follow experiments.

Fig. 2 depicted the effect of rabbit serum dilution in the IgG attachment yield. From Fig. 2 and SE-HPLC chromatograms (Figure S2, Supporting Information), it can be concluded that rabbit serum dilutions lower than 1:20 (1:5 and 1:15) lead to lower IgG attachment yields of 50.5% and 58.0%, respectively. On the other hand, increased rabbit serum dilutions (1:20, 1:30 and 1:50) are advantageous, with an 100% IgG attachment on the MWCNTs, since no IgG peak is observed in the SE-HPLC chromatograms (Figure S2, Supporting Information). These results reveal that lower total protein concentrations (higher dilutions) favors the attachment of IgG present in rabbit serum, indicating a preferential adsorption capacity of IgG on the surface of the MWCNTs. In fact, according to the SE-HPLC chromatograms (Supporting Information, Figure S2), RSA (naturally present in rabbit serum)is also attached to the MWCNTs (Table S3 in the Supporting Information), reducing the IgG attachment for lower serum dilutions of 1:5 and 1:15 (RSA attachment yield of 45.9% and 40.6%, respectively). On the other hand, for higher serum dilutions of 1:20, 1:30 and 1:50, a RSA attachment yield of 35.8%, 41.2%, and 67.8% was obtained, respectively (Table S3 in the Supporting Information). Besides the increase in RSA attachment yield, the amount of RSA attached did not increase due to the serum dilution increase. Considering the RSA concentration of 35 mg/mL and the volume of serum used in each serum dilution, the amount of RSA attached to the MWCNTs was estimated as 321.3 μg, 94.8 μg, 62.6 μg, 48.1 μg and 47.5 μg for serum dilutions of 1:5, 1:10 1:20, 1:30 and 1:50, respectively (Table S3 in the Supporting Information). The attachment of RSA at these higher serum dilutions had no effect on the IgG attachment. In summary, it is possible to conclude that the serum dilution decreased the capacity of MWCNTs in adsorb other proteins from rabbit serum while increasing the IgG yield to 100%.

Moreover, by estimating the number of IgG that the MWCNTs can adsorb (Supporting Information, Table S4), it is possible to verify that, in theory, the MWCNTs with an external diameter of 10-20 nm have enough adsorption capacity for the total IgG molecules present in the initial samples of diluted rabbit serum. However, as previously mentioned, the presence of other proteins could hinder the IgG attachment.

Based on the results, the MWCNTs with an external diameter of 10-20 nm and a rabbit serum dilution of 1:20 (maximum concentration of total protein leading to an IgG attachment yield of 100%) were selected for further assays.

To investigate the impact of MWCNTs surface chemistry on the IgG attachment, different functionalization approaches were applied to pristine MWCNTs surface. Non-functionalized MWCNTs (control); MWCNTs functionalized by a hydrothermal route with HNO_3 (7M) at 130°C (MWCNTox); and MWCNTox treated under an inert atmosphere (N_2) at 400°C (MWCNTox 400) and at 900°C (MWCNTox 900) were used [18].

Oxygenated functional groups can be formed spontaneously by exposure of carbon materials to the atmosphere. Nevertheless, the concentration is normally very low and can be further increased by oxidative treatment. Aditionally, it has been reported that the oxidation treatment with HNO_3 produces materials with large amounts of surface acidic groups, mainly carboxylic acids and, to a smaller extent, lactones, anhydrides, and phenol groups formed at the edges/ends and defects of graphitic sheets. The different surface oxygenated groups decompose by heating at determined temperatures. Carboxylic acids, for example, are removed by heating at 400 °C and nearly total removal of surface groups is observed after treating MWCNTox at 900 °C [18,30-32]. The surface chemistry of the MWCNTs used in this work, namely temperature-programmed desorption (TPD) profiles, are shown in previous studies [18].

In this work, 2 mg of each MWCNTs, a rabbit serum dilution of 1:20 (in 0.15 M citrate/phosphate buffer pH 5.0) and 60 min of contact were the adsorption conditions applied. According to Fig. 3, it is possible to observe that the best IgG attachment yield (100%) occurred for pristine MWCNTs, i.e. without any functionalization.

The treatment of MWCNTox with higher temperatures led to lower IgG attachment yields (55.1% - 5.0%). This behavior between the non-functionalized MWCNTs and the modified MWCNTs may foresee the existence of distinct interaction mechanisms between IgG and both materials. In the case of the pristine material, since no defects were created at the surface of the CNTs, hydrophobic and $\pi - \pi$ stacking interactions are the most probable mechanisms of IgG interaction. IgG from rabbit serum contains hydrophobic regions on its structure, which may lead to an adsoption on the external walls of MWCNTs through hydrophobic interactions. On the other hand, $\pi - \pi$ stacking interactions

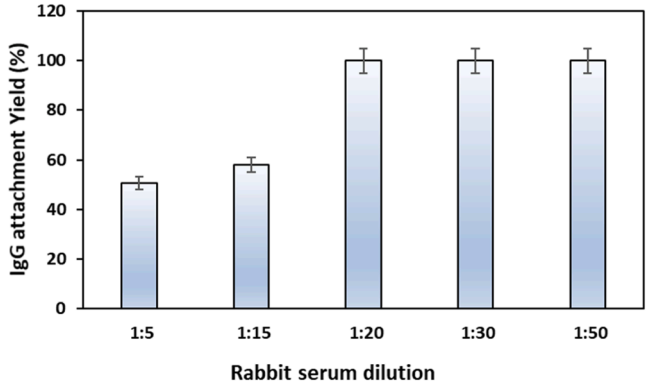

Fig. 2. Effect of rabbit serum dilution in the attachment of IgG present in rabbit serum using 2 mg of MWCNTs (external diameter of 10-20 nm) during 60 min of contact time, pH 5.0.

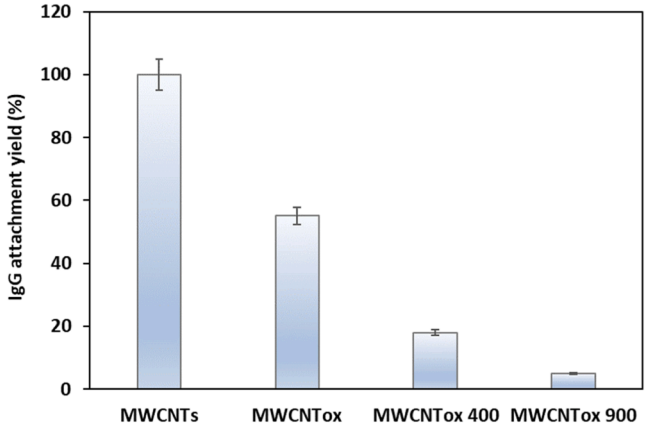

Fig. 3. Effect of MWCNTs functionalization in the attachment of IgG present in rabbit serum using 2 mg of MWCNTs (external diameter of 10-20 nm) and a rabbit serum dilution of 1:20, pH 5 and 60 min of contact time.

between the sidewalls of pristine MWCNTs and the aromatic residues on the structure of IgG may also contribute to the interaction with the materials. For the functionalized materials, the differences in IgG attachment performance can be mostly attributed to the existence of electrostatic interactions between the support and the antibody. Attachment yields are in agreement with the charge properties of MWCNTox and IgG which means the pH of the point of zero charge (pH_{PZC}) of the carbon materials (determined by Silva et al. [18]) and the isoelectric point of IgG (pI ranges between 5.3-7.1 [33]. Thus, among the modified materials, at pH 5.0 MWCNTox 900 presents the lowest IgG attachment yield (5.0%), which may be related to the positive charge of the material (pH_{PZC} of MWCNTox 900 = 6.9 [18]) and the positive charge of IgG, leading to repulsive interactions. Regarding the other materials (MWCNTox and MWCNTox 400), IgG attachments yields of 55.1 and 18% were obtained. In this case, at pH 5.0, both materials are negatively charged (pH_{PZC} of MWCNTox = 3.0; pH_{PZC} of MWCNTox 400 = 4.0 [18]) and IgG is positively charged, contributing to the existence of electrostatic interactions between the material and the antibody.

Fig. 4 shows a TEM micrograph of pristine MWCNTs (Fig. 4a) and the IgG@MWCNT bioconjugate (Fig. 4b) where is notorious the presence of IgG particles at the sidewalls of the carbon nanotubes.

To confirm the interaction mechanisms between IgG and MWCNTs, a computational protonation analysis of the amino acids of the IgG chains was performed from pH 5.0 to 8.0. The electrostatic charge of the IgG surface is depicted in Fig. 5. According to the results, at pH 5.0 the antibody surface shows a balance between positive and negative charges (blue and red in Fig. 5, respectively). As expected, with a pH increase, from 5.0 to 6.0, there is a decrease of positively charged amino acids, becoming deprotonated. Additionally, an increase in the number of negatively charged amino acids can be observed. From pH 6.0 to 7.0 a slight modification of the surface charge of the amino acids of the antibody can be visualized. The same behavior was found by increasing the pH from 7.0 to 8.0. The reported pI of IgG ranges between 5.3-7.1 [33], so the increase of negatively charged amino acids is expected, since the proteins are negatively charged above their isoelectric point.

Subsequently, after the calculation of IgG protonation, the reactive potential of each amino acid at pH 5.0 to 8.0 was performed. For this, the amino acids that were available on the surface of the antibody were evaluated (excluding buried amino acids, which possibly do not interact with the MWCNTs). The amino acids that have the ε-amino group (Lysine (LYS) and NH_2-terminal end (N-term)) were selected and amino acid reactivity (*LIGRe*) was calculated. The *LIGRe* values for the N-term amino acids are available in Table 1, while the *LIGRe* for LYS amino acids are shown in supporting information (Supporting Information, Table S5). In general, *LIGRe* values increase with increasing pH, following the rank: 5.0 <6.0 <7.0 <8.0. At pH 5.0 and 6.0, all amino acids analyzed showed non-reactivity potential (*LIGRe* < 0.1). The reactivity values increase at pH 7.0, where 3 N-term amino acids are half-reactive (0.1 < *LIGRe* < 1.0). Finally, at pH 8 IgG N-term amino acids are considered reactive (*LIGRe* ≥ 1.0). Only N-term amino acids showed potential reactivity, while all LYS amino acids showed no reactivity at all pHs studied. With the acquired information it is possible to visualize the regions of IgG that interact with MWCNTs.

The identification of the N-term reactive at pH 8.0 is depicted in Fig. 6. After identification, it noticeable that 2 N-term amino acids are located at IgG heavy chain and 1 N-term in the light chain, being the N-term of heavy chain the most reactive. Therefore, the possible orientation of the antibody on the carbon nanotube surface is described as "end-on". Moreover, it is important to mention that since the amount of RSA attached to MWNT decreased rapidly with serum dilution, no RSA effect on LIGRe and orientation is expected. This orientation of the antibody on the solid carrier is based on the interaction between the Fc fragment, preserving the Fab fragment for antigen recognition. The orientation of antibody was also investigate by the adsorption of IgG on high affinity carboxylated/oxidized nanodiamonds [28]. IgG immobilization on the surface of nanodiamonds was based on interactions with material active functional group with IgG amino acids residues. The presence of more carboxyl groups allowed the enhancement of IgG adsorption (three times higher), in comparison with non-air-oxidized nanodiamonds [28]. The immobilization of pure mouse IgG onto CNTs trough covalent and non-covalent was also carried out by Wallace and co-workers [34]. The authors evaluated the ability of IgG immobilized as electrochemical transducer using both immobilization approaches. The covalent immobilized IgG displayed electrochemically detectable labelled antibodies on the CNTs surface, showing the potential application for immunoassays devices. Oriented attachment of IgGs was performed by Guisán and co-workers [35], and "end-on" strategy applied allows the improvement on antigen recognition in comparison with random attachment protocol, even in recognition of analytes in biological samples (complex matrices). Based on this, the IgG oriented attachment in MWCNT developed here presented could be an effective strategy to maintain antibody able to antigen recognition, and to be applied for biomedical applications.

Based on the previous results of *LIGRe*, and in order to improve the IgG attachment yield on the functionalized MWCNTs, MWCNTox were selected for the evaluation of the pH effect, since this material was the

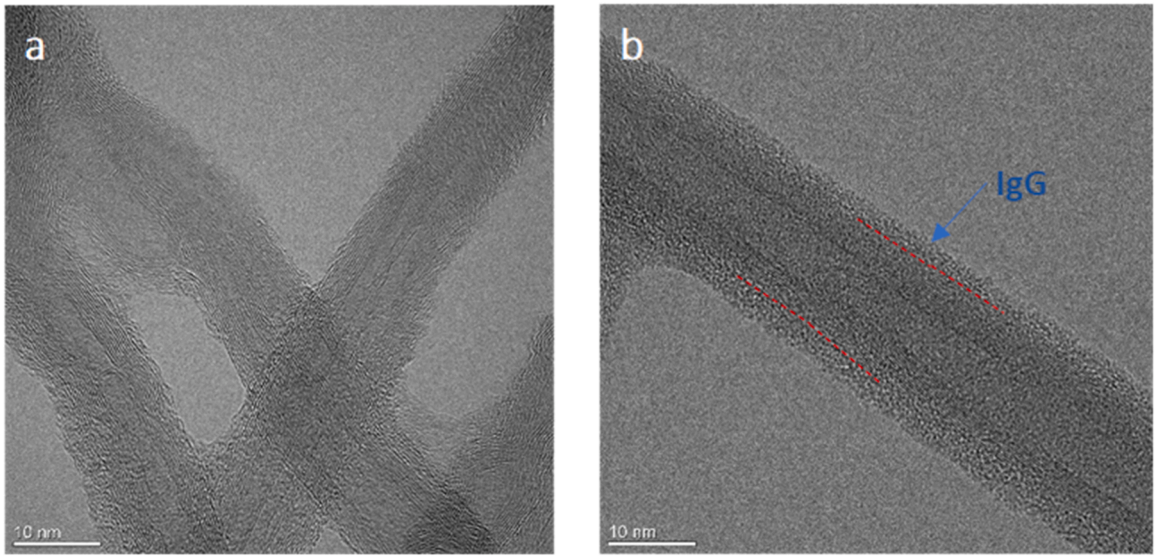

Fig. 4. TEM images of the MWCNT before (a) and after (b) IgG adsorption on its sidewalls.

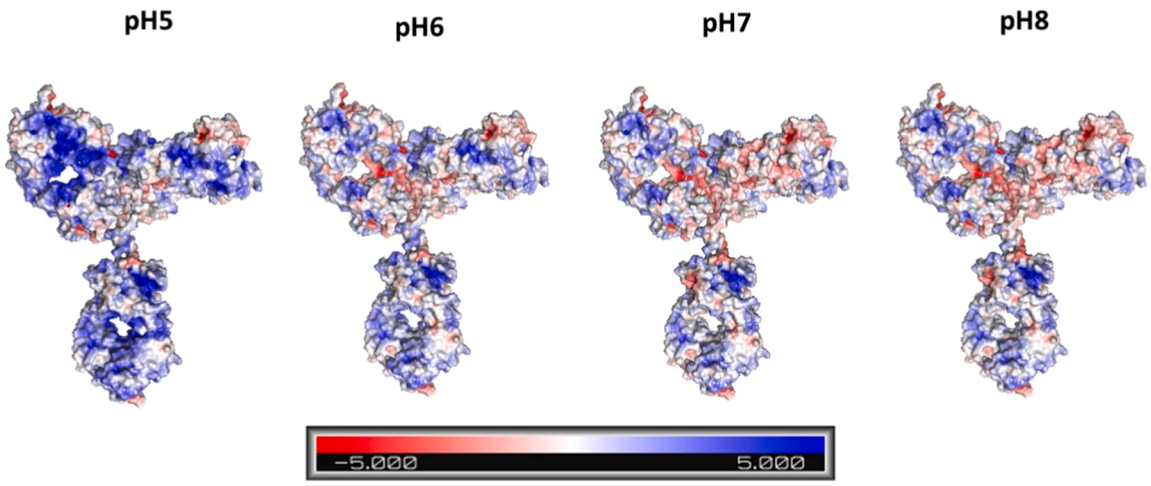

Fig. 5. Electrostatic surface charge at the IgG surface calculated for pH range: from 5.0 to 8.0. Red-white-blue scale refers to minimum (-5 kT/e, red) and maximum (5 kT/e, blue) surface potential.

Table 1
Amino acid reactivity (*LIGRe)* for IgG: from pH 5.0 to 8.0.

Amino acid residue	Chain	pK_a	LIGRe pH 5.0	pH 6.0	pH 7.0	pH 8.0
N-Term	H	7.70	0.00	0.02	0.20	2.00
N-Term	K	7.76	0.00	0.02	0.17	1.74
N-Term	L	8.05	0.00	0.01	0.09	0.89
N-Term	M	7.97	0.00	0.01	0.11	1.07

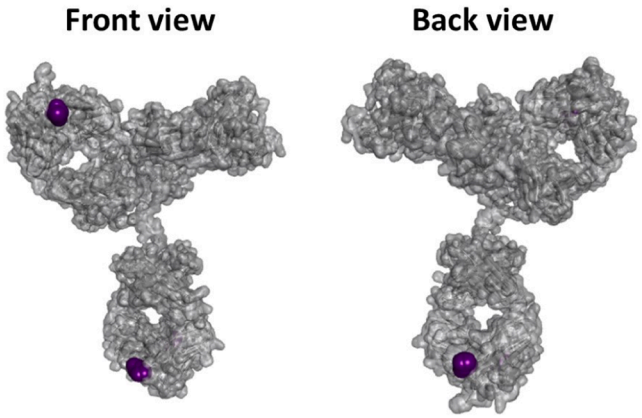

Fig. 6. Surface visualization of IgG structure showing N-Term reactive groups at pH 8.0.

most promising functionalized MWCNTs. To evaluate the pH effect, 2 mg MWCNTox, rabbit serum dilution of 1:20 (in different buffers in a pH range between 5.0 and 8.0) and 60 min of contact were applied. The results of IgG attachment yield on the material are depicted in Fig. 7. In all the assays, the material is negatively charged since the pH_{PZC} of MWCNTox = 3.0 [18], while IgG is increasing its negative charge with the increase of pH (pI ranges between 5.3-7.1 [33]). Although the increase of the pH, a decrease in the attachment yield would be expected due to repulsive electrostatic interactions, an opposite behavior was observed. IgG attachment yields of 100 % were obtained for assays at pH range between 6.0 and 8.0, revealing that indeed electrostatic interaction doesn't rule the adsorption of IgG on the material.

Different authors have been reported studies on the antibodies and proteins conjugation with CNTs, for different applications, and using various types of CNTs and antibodies [16,20,23]. In particular, the work

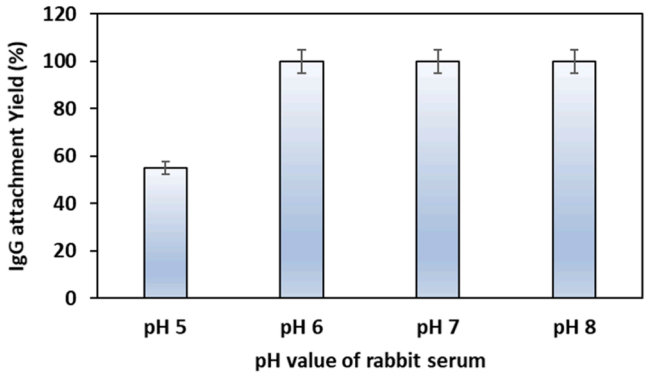

Fig. 7. Effect of pH value of rabbit serum in the attachment of IgG present in rabbit serum using 2 mg of MWCNTox (external diameter of 10-20 nm) and a rabbit serum dilution of 1:20, during 60 min of contact time.

by Zhang et al [36], described the effect MWCNTs surface chemistry in the adsorption of pure bovine serum albumin (BSA) and pure IgG at a fixed concentration of 0.2 mg/mL. It was found that the adsorption capacity was dependent on the properties of MWCNTs. Comparing with the present work, a complex biological matrix containing IgG and albumin was used in addition to the evaluation of MWCNTs external diameter. Thus, for the best of our knowledge, all these studies used pure monoclonal antibodies or pure proteins. In this work we report the efficient IgG attachment (100%) in MWCNTs from a complex biological matrix (rabbit serum), which includes other naturally present proteins, namely RSA. Additionally, the IgG present in this complex matrix is a polyclonal antibody, meaning that display multi-epitope binding properties, which make it ideally suited for many applications, namely for assay-specific target discovery and detection [37].

3.2. *Evaluation of the desorption of Immunoglobulin G from MWCNTox*

To prove the strong interaction between the IgG and the MWCNTs, and the potential of this bioconjugate for biomedical applications, different assays were performed to verify if IgG can be easily desorbed or not from the MWCNTox (at this condition an IgG attachment yield was obtained). All the experimental conditions performed, and results are resumed in Table 2.

Initially, 0.15 M citrate/phosphate buffer at different pH values (pH 4, pH 5 and pH 6), 0.2 M phosphate buffer (pH 7 and pH 8) and 0.5 M carbonate buffer (pH 9 and pH 11) were used. Since the isoelectric point

Table 2
Experimental conditions applied to promote the desorption of IgG from MWCNTox.

Assay	Solvent	pH	Concentration (M)	IgG desorption
1	0.15 M citrate/phosphate	4.0 5.0 6.0	-	×
2	0.2 M phosphate buffer	7.0 8.0	-	×
3	0.5 M carbonate buffer	9.0 11.0	-	×
4	Phosphate buffer saline	7.4	-	×
5	NaCl aqueous solution		1.0 1.5 2.0 2.5	×
6	0.15 M citrate/phosphate with NaCl	2.8	0.5	×
7	Water with HCl	2.8	-	×

of IgG varies between 5.3 and 7.1 [33] with a electrostatic charge varying with pH values (Fig. 5) and the pH_{PZC} of MWCNTox is 3.0 [18], using buffers with pH values between 4.0 and 11.0, different density charges of the antibody and the material occurred. For instance, at pH values higher than 7.0, the antibody and the material are negatively charge, so repulsive interactions may occur. However, at the experimental conditions tested, the desorption of IgG from the MWCNTox did not occur, and as described above, other interactions such as hydrophobic and $\pi - \pi$ stacking interactions are the most probable mechanisms of IgG attachment.

The use of PBS was also evaluated. This buffer is biocompatible, and it was intended to desorb the IgG from the material through direct contact. However, it was verified that the addition of PBS was also not effective.

Then, the effect of NaCl aqueous solutions (1.0, 1.5, 2.0 and 2.5 M) was evaluated. The selection of this salt was made on the basis of a previous study from the literature [38], in which the recovery of IgG from human serum was from 0% to 95% when increasing the concentration of NaCl from 0.01 M to 2.0 M. Nevertheless, this attempt was also not successful since IgG remained adsorbed on the MWCNTox.

Trying a new approach, 0.1 M citrate/phosphate buffer at pH 2.8 with 0.5 M NaCl was tested. The addition of NaCl to the buffer had the objective of removing the electrostatic interactions between IgG and the MWCNTox. However, it was not possible to detect IgG in solution after the desorption process, so the IgG remained linked to the material.

As a last attempt, aqueous NaCl solution at pH 12.0 and water with HCl at pH 2.8 were tested to try remove the main protein-protein and antibody-antigen binding interactions without permanently affecting protein structure. Nonetheless, IgG was detected in the supernatant and the desorption did not occur.

Based on these results, the interaction between IgG and MWCNTox is very strong in different aqueous environments at different pH values and salts concentrations and its application in biomedical area and as a biosensor is very promising.

4. Conclusions

MWCNTs are promising nanomaterials for the adsorption and attachment of IgG from rabbit serum for biomedical applications. Using pristine MWCNTs with an external diameter ranging between 10-20 nm and higher dilutions of rabbit serum, IgG attachment yields of 100% were obtained, while other proteins attachemnet, namely RSA, decreased. Moreover, different reactive N-term in the antibody at pH 8.0 were identified by a computational analysis, and an “end-on” orientation of the antibody on the MWCNTs surface was described. Furthermore, the presence of a small amount of other proteins at higher serum dilutions has no effect on IgG activity or orientation. This orientation of the antibody on the solid carrier demonstrated that the IgG oriented attachment in MWCNTs developed here presented could be an effective strategy to maintain antibody able to antigen recognition, and to be applied for biomedical applications. Finally, the desorption of IgG from MWCNTs was evaluated using different strategies. None of the strategies applied were successful, reinforcing the strong interaction between the antibody and the nanomaterial, and its potential in the biomedical field.

Declaration of Competing Interest

The authors declare that they have no known competing financial interests or personal relationships that could have appeared to influence the work reported in this paper.

Data availability

Data will be made available on request.

Acknowledgements

This work was developed within the scope of the project CICECO-Aveiro Institute of Materials, UIDB/50011/2020, UIDP/50011/2020 & LA/P/0006/2020, financed by national funds through the FCT/MEC (PIDDAC). This work was also financially supported by LA/P/0045/2020 (ALiCE), UIDB/50020/2020 and UIDP/50020/2020 (LSRE-LCM), funded by national funds through FCT/MCTES (PIDDAC), and POCI-01-0145-FEDER-031268—funded by FEDER, through COMPETE2020—Programa Operacional Competitividade e Internacionalização (POCI), and by national funds (OE), through FCT/MCTES. Ana P. M. Tavares acknowledges the FCT for the research contract CEECIND/2020/01867. Rita A. M. Barros acknowledges FCT for her PhD grant 2022.12055.BD.

Supplementary materials

Supplementary material associated with this article can be found, in the online version, at doi:10.1016/j.cep.2022.109214.

References

[1] D Tasis, N Tagmatarchis, A Bianco, M. Prato, Chemistry of carbon nanotubes, Chem. Rev. 106 (2006) 1105–1136, https://doi.org/10.1021/cr050569o.
[2] P-C Ma, NA Siddiqui, G Marom, J-K. Kim, Dispersion and functionalization of carbon nanotubes for polymer-based nanocomposites: a review, Compos. Part A Appl. Sci. Manuf. 41 (2010) 1345–1367, https://doi.org/10.1016/j.compositesa.2010.07.003.
[3] A Dettlaff, M Sawczak, E Klugmann-Radziemska, D Czylkowski, R Miotk, M. Wilamowska-Zawłocka, High-performance method of carbon nanotubes modification by microwave plasma for thin composite films preparation, RSC Adv. 7 (2017) 31940–31949, https://doi.org/10.1039/C7RA04707J.
[4] X Dong, C Wei, J Liang, T Liu, D Kong, F. Lv, Thermosensitive hydrogel loaded with chitosan-carbon nanotubes for near infrared light triggered drug delivery, Colloids Surf. B Biointerfaces 154 (2017) 253–262, https://doi.org/10.1016/j.colsurfb.2017.03.036.
[5] SK Verma, A Modi, J. Bellare, Polyethersulfone-carbon nanotubes composite hollow fiber membranes with improved biocompatibility for bioartificial liver, Colloids Surf. B Biointerfaces 181 (2019) 890–895, https://doi.org/10.1016/j.colsurfb.2019.06.051.
[6] VR Raphey, TK Henna, KP Nivitha, P Mufeedha, C Sabu, K. Pramod, Advanced biomedical applications of carbon nanotube, Mater. Sci. Eng. C 100 (2019) 616–630, https://doi.org/10.1016/j.msec.2019.03.043.
[7] G Tejendra Kumar, B Pattabhi Ramaiah, C Sivakumar Reddy, YB Sudhir Sastry, P Marco, PB Stephane, Advances in carbon based nanomaterials for Bio-medical applications, Curr. Med. Chem. 26 (2019) 6851–6877, https://doi.org/10.2174/0929867326666181126113605.
[8] G Hong, S Diao, AL Antaris, H. Dai, Carbon nanomaterials for biological imaging and nanomedicinal therapy, Chem. Rev. 115 (2015) 10816–10906, https://doi.org/10.1021/acs.chemrev.5b00008.
[9] G Lalwani, AM Henslee, B Farshid, L Lin, FK Kasper, Y-X Qin, et al., Two-dimensional nanostructure-reinforced biodegradable polymeric nanocomposites

for bone tissue engineering, Biomacromolecules 14 (2013) 900–909, https://doi.org/10.1021/bm301995s.
[10] M Arruebo, M Valladares, Á. González-Fernández, Antibody-conjugated nanoparticles for biomedical applications, J Nanomater 2009 (2009), 439389, https://doi.org/10.1155/2009/439389.
[11] D Pantarotto, CD Partidos, J Hoebeke, F Brown, E Kramer, J-P Briand, et al., Immunization with peptide-functionalized carbon nanotubes enhances Virus-specific neutralizing antibody responses, Chem. Biol. 10 (2003) 961–966, https://doi.org/10.1016/j.chembiol.2003.09.011.
[12] AA Chaudhari, D Ashmore, Kate K Nath S deb, V Dennis, SR Singh, et al., A novel covalent approach to bio-conjugate silver coated single walled carbon nanotubes with antimicrobial peptide, J. Nanobiotechnol. 14 (2016) 58, https://doi.org/10.1186/s12951-016-0211-z.
[13] V Zubkovs, S-J Wu, SY Rahnamaee, N Schuergers, AA. Boghossian, Site-specific protein conjugation onto fluorescent single-walled carbon nanotubes, Chem. Mater. 32 (2020) 8798–8807, https://doi.org/10.1021/acs.chemmater.0c02051.
[14] W Huang, S Taylor, K Fu, Y Lin, D Zhang, TW Hanks, et al., Attaching proteins to carbon nanotubes via diimide-activated amidation, Nano Lett. 2 (2002) 311–314, https://doi.org/10.1021/nl010095i.
[15] Y-S Lo, DH Nam, H-M So, H Chang, J-J Kim, YH Kim, et al., Oriented immobilization of antibody fragments on Ni-decorated single-walled carbon nanotube devices, ACS Nano 3 (2009) 3649–3655, https://doi.org/10.1021/nn900540a.
[16] TS Huang, Y Tzeng, YK Liu, YC Chen, KR Walker, R Guntupalli, et al., Immobilization of antibodies and bacterial binding on nanodiamond and carbon nanotubes for biosensor applications, Diam. Relat. Mater. 13 (2004) 1098–1102, https://doi.org/10.1016/j.diamond.2003.11.047.
[17] Almeida MR, Cristóvão RO, Barros MA, Nunes JCFF, Boaventura RARR, Loureiro JM, et al. Superior operational stability of immobilized l-asparaginase over surface-modified carbon nanotubes 2021;11. doi:10.1038/s41598-021-00841-2.
[18] CG Silva, APM Tavares, G Dražić, AMT Silva, JM Loureiro, JL. Faria, Controlling the surface chemistry of multiwalled carbon nanotubes for the production of highly efficient and stable laccase-based biocatalysts, Chempluschem 79 (2014), https://doi.org/10.1002/cplu.201402054.
[19] A Shankar, J Mittal, A. Jagota, Binding between DNA and carbon nanotubes strongly depends upon sequence and chirality, Langmuir 30 (2014) 3176–3183, https://doi.org/10.1021/la500013c.
[20] R Li, R Wu, L Zhao, M Wu, L Yang, H. Zou, P-glycoprotein antibody functionalized carbon nanotube overcomes the multidrug resistance of human leukemia cells, ACS Nano 4 (2010) 1399–1408, https://doi.org/10.1021/nn9011225.
[21] R Marches, P Chakravarty, IH Musselman, P Bajaj, RN Azad, P Pantano, et al., Specific thermal ablation of tumor cells using single-walled carbon nanotubes targeted by covalently-coupled monoclonal antibodies, Int. J. Cancer 125 (2009) 2970–2977, https://doi.org/10.1002/ijc.24659.
[22] P Chakravarty, R Marches, NS Zimmerman, ADE Swafford, P Bajaj, IH Musselman, et al., Thermal ablation of tumor cells with antibody-functionalized single-walled carbon nanotubes, Proc. Natl. Acad. Sci. U. S. A. 105 (2008) 8697–8702, https://doi.org/10.1073/pnas.0803557105.
[23] E Venturelli, C Fabbro, O Chaloin, C Ménard-Moyon, CR Smulski, T Da Ros, et al., Antibody covalent immobilization on carbon nanotubes and assessment of antigen binding, Small 7 (2011) 2179–2187, https://doi.org/10.1002/smll.201100137.
[24] CC Ramalho, CMSS Neves, M V Quental, JAP Coutinho, MG. Freire, Separation of immunoglobulin G using aqueous biphasic systems composed of cholinium-based ionic liquids and poly(propylene glycol), J. Chem. Technol. Biotechnol. 93 (2018) 1931–1939, https://doi.org/10.1002/jctb.5594.
[25] G Martínez-Rosell, T Giorgino, G. De Fabritiis, PlayMolecule ProteinPrepare: a web application for protein preparation for molecular dynamics simulations, J. Chem. Inf. Model. 57 (2017) 1511–1516, https://doi.org/10.1021/acs.jcim.7b00190.
[26] P Torres-Salas, A del Monte-Martinez, B Cutiño-Avila, B Rodriguez-Colinas, M Alcalde, AO Ballesteros, et al., Immobilized biocatalysts: novel approaches and tools for binding enzymes to supports, Adv. Mater. 23 (2011) 5275–5282, https://doi.org/10.1002/adma.201101821.
[27] H Tsai, YH Lu, HX Liao, SW Wu, FY Yu, CB. Fuh, Detection of rabbit IgG by using functional magnetic particles and an enzyme-conjugated antibody with a homemade magnetic microplate, Chem. Cent. J. 9 (2015), https://doi.org/10.1186/S13065-015-0088-1.
[28] AA Patil, MJN Descanzo, JBA Agcaoili, C-K Chiang, C-L Cheng, H-C Chang, et al., Carboxylated/Oxidized diamond nanoparticles for quantifying immunoglobulin g antibodies using mass spectrometry, ACS Appl. Nano Mater. 4 (2021) 8922–8936, https://doi.org/10.1021/acsanm.1c01553.
[29] N Saifuddin, AZ Raziah, AR. Junizah, Carbon nanotubes: a review on structure and their interaction with proteins, J. Chem. 2013 (2013), 676815, https://doi.org/10.1155/2013/676815.
[30] JL Figueiredo, MFR. Pereira, The role of surface chemistry in catalysis with carbons, Catal. Today 150 (2010) 2–7, https://doi.org/10.1016/J.CATTOD.2009.04.010.
[31] JL Figueiredo, MFR Pereira, MMA Freitas, JJM. Órfão, Modification of the surface chemistry of activated carbons, Carbon N Y 37 (1999) 1379–1389, https://doi.org/10.1016/S0008-6223(98)00333-9.
[32] JL Figueiredo, MFR Pereira, MMA Freitas, JJM. Órfão, Characterization of active sites on carbon catalysts, Ind. Eng. Chem. Res. 46 (2006) 4110–4115, https://doi.org/10.1021/IE061071V.
[33] MA Clauss, RK. Jain, Interstitial transport of rabbit and sheep antibodies in normal and neoplastic tissues, Cancer Res. 50 (1990) 3487–3492.
[34] C Lynam, N Gilmartin, AI Minett, R O'Kennedy, G. Wallace, Carbon nanotube-based transducers for immunoassays, Carbon N Y 47 (2009) 2337–2343, https://doi.org/10.1016/j.carbon.2009.04.017.
[35] S Gao, F Rojas-Vega, J Rocha-Martin, JM. Guisán, Oriented immobilization of antibodies through different surface regions containing amino groups: Selective immobilization through the bottom of the Fc region, Int. J. Biol. Macromol. 177 (2021) 19–28, https://doi.org/10.1016/j.ijbiomac.2021.02.103.
[36] T Zhang, M Tang, Y Yao, Y Ma, Y. Pu, MWCNT interactions with protein: surface-induced changes in protein adsorption and the impact of protein corona on cellular uptake and cytotoxicity, Int. J. Nanomed. 14 (2019) 993, https://doi.org/10.2147/IJN.S191689.
[37] CA Ascoli, B. Aggeler, Overlooked benefits of using polyclonal antibodies, BioTechniques 65 (2018) 127–136, https://doi.org/10.2144/btn-2018-0065.
[38] Z Du, S Zhang, C Zhou, M Liu, G. Li, l-histidine functionalized multi-walled carbon nanotubes for on-line affinity separation and purification of immunoglobulin G in serum, Talanta 99 (2012) 40–49, https://doi.org/10.1016/j.talanta.2012.05.018.